Soil Dynamics and Earthquake Engineering xxx (xxxx) xxx–xxx

Contents lists available at ScienceDirect

Soil Dynamics and Earthquake Engineering

journal homepage: www.elsevier.com/locate/soildyn

Development of hazard- and amplification-consistent elastic design spectra

Valerio Poggi[a,b,*], Benjamin Edwards[a,c], Donat Fäh[a]

[a] Swiss Seismological Service, Institute of Geophysics, ETH Zurich, Switzerland
[b] Global Earthquake Model foundation (GEM), Pavia, Italy
[c] Department of Earth, Ocean and Ecological Sciences, University of Liverpool, United Kingdom

ARTICLE INFO

Keywords:
Site amplification
Design spectra
Spectral modeling
Seismic hazard
Vs_{30}

ABSTRACT

In the framework of the definition of a new building code for dams, the Swiss Federal Office for Energy (SFOE) has commissioned a study on the effect of site response variability on elastic design spectra for different soil conditions and seismic hazard scenarios. The goal of the study presented herein is the definition of a new set of site-dependent design spectra for horizontal and vertical ground-motion, whose design shape (scaled to peak ground acceleration) is to be compared with the present Swiss normative (SIA261, revision 2014) [43].

To accomplish the task, we have created a large dataset of Fourier-domain seismic amplification functions by collecting empirical observations and site-specific ground motion models from both measured and stochastically generated velocity profiles. Fourier spectra were then converted to response spectral amplification using a combination of spectral modeling techniques and random vibration theory. Average amplification models are thus derived for different soil classes (SIA class A–E), according to the Swiss building code provisions, and for a set of magnitude-distance combinations chosen as representative of the Swiss hazard disaggregation scenario at the Sion site in Switzerland.

Finally, the response spectral amplification functions from the database have been combined with the normalized uniform hazard spectra computed at Sion for return periods of 500, 1000, 5000 and 10,000 years. Based on those results, a new set of design spectral shapes is proposed for the different SIA soil classes, accounting for investigated scenario variability and including a reasoned level of conservatism dependent on the distribution of the site-specific amplification models.

The proposed methodology targets the reduction in uncertainty associated with seismic design and, although originally focused and applied to the Swiss norm, it could be potentially applied to any national seismic code as a tool for developing, updating or benchmarking the current provisions in a holistic framework.

1. Introduction

Elastic design spectra (EDS) represent a solution to the need of simplifying the description of the seismic design force demand of structures subject to an arbitrary ground motion level [25,33]. In current engineering practice, national building codes prescribe the functional form of the elastic design spectrum for a number of simplified soil classes (e.g. [10,15,26]). Normative design spectra are natively non-dimensional and must be subsequently scaled to a reference intensity level (e.g. peak ground acceleration, PGA) defined for a given probability of exceedance and investigation time (in general 50 years).

In spite of their simple usage, the calibration of EDS is not trivial and requires the statistical analysis of large sets of earthquake recordings to cover the broad variability of controlling parameters such as magnitude, distance and soil conditions [8]. Unfortunately, the availability of empirical data is generally limited [7], particularly for low seismicity region or where an adequate seismic network is not available. To overcome this limitation, calibration data are often imported from external datasets. This approach, however, could introduce bias due to the potential mismatch of seismic characteristics (e.g. path attenuation, tectonic style) between the host (external) and the target (local) regions. To address these limitations, adjustments are necessary, such as amplitude scaling and spectral modulation (e.g. [1,2]). These procedures introduce further uncertainty and can result in correlations within calibration data.

The lack of information is particularly critical when it comes to the level of site-specific analysis [42], due both to the substantial lack of recordings to characterize the large range of possible site conditions and to the limited availability of high-quality site-specific studies at the location of seismic stations. Moreover, the use of oversimplified soil classification schemes, often relying on a single parameter such as the widely used travel-time average velocity over the topmost 30 m (Vs_{30};

* Corresponding author at: Global Earthquake Model foundation (GEM), Pavia, Italy.
E-mail address: valerio.poggi@globalquakemodel.org (V. Poggi).

https://doi.org/10.1016/j.soildyn.2018.03.011
Received 8 July 2017; Received in revised form 14 December 2017; Accepted 9 March 2018

[9,17,16]), imposes severe limitations in depicting the complexity of the site response. As a result, elastic design spectra might deviate from observations [34], in few cases significantly.

In recent years the scientific and engineering communities have paid increasing attention to the influence of local site conditions on the modification of the ground motion. Progress was due in part to the development of new and more reliable site characterization techniques and in part to the availability of a new generation of seismic networks with recordings in free-field conditions (e.g. [31,39]). Regrettably, the long validation time required and the need for stability over relatively long periods have considerably delayed the update of the seismic design provisions in this regard (e.g. [44]).

Target of this study is to highlight the need to update the current building codes to better account for site-specific response in EDS provisions. To do that, we examined the influence of a large set of realistic ground-motion amplification models for different soil conditions on class-specific normalized design spectra, defined for both the horizontal and the vertical components. This analysis has been commissioned by the Swiss Federal Office for Energy (SFOE) in the context of the renewal of the building code for dams. Although our focus is on the soil classification according to the Swiss Building Code [43], the considerations presented thereinafter have general implications to any seismic provision, such as the Eurocode 8 [15] and NEHRP [10].

2. Methodology

It is impractical to use site-specific response spectra from earthquake recordings to map the large variability of site conditions. This is due to the limited amount of data usually available for the different soil classes. In this study, we therefore use an alternative strategy based on the combination of information from probabilistic seismic hazard analysis and site-specific amplification functions from direct observations and modeling methods (Fig. 1).

In a first step, a large database of site-specific Fourier amplification spectra (FAS) is obtained by combining empirical observations of earthquake recordings and estimates from different modeling strategies, such as a predictive empirical model [37], based on the comparison between actual observations and quarter-wavelength average soil parameters [27], and the one-dimensional SH-wave transfer function. Modeled amplification functions are computed from a collection of one-dimensional shear-wave velocity profiles, which includes sites from the Swiss (strong motion: SSMNet, broadband: SDSNet) and Japanese (KiKNet) seismic networks. A set of stochastically generated soil models is

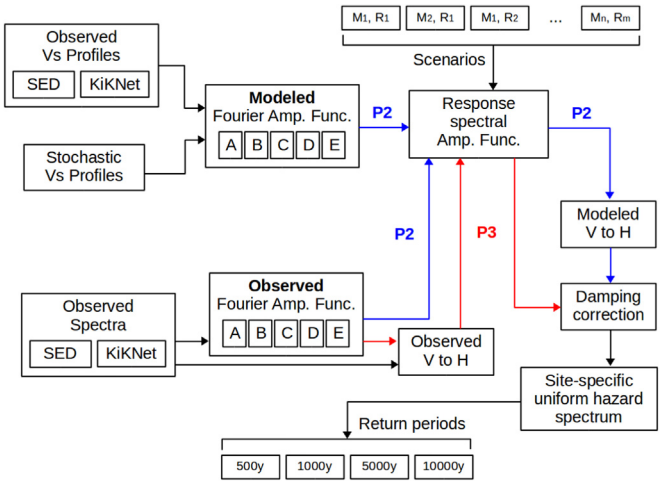

Fig. 1. Schematic representation of the processing tree to compute site-specific uniform hazard spectra for the vertical and horizontal component combining different strategies.

Table 1
Vs_{30} upper and lower bounds (units in m/s) for the definition of SIA 261 classes used in this study. It is important to stress that, while sharing some similarities, SIA soil classification is noticeable different from EC8.

Class	Vs_{30} Min. (m/s)	Vs_{30} Max. (m/s)	Thickness (m)	Description
A	800	2500	< 5 (soil cover)	Hard rock (with optional soil cover)
B	500	800	> 30	Consolidated gravel/sand
C	300	500	> 30	Non consolidated gravel/sand
D	100	300	> 30	Non consolidated fine sand/silt
E	100	500	5–30	Soft sediments (class C or D) over a stiff bedrock (class A or B)

also added to represent the full range of possible velocity profiles in specific soil classes. Empirical amplification functions are obtained by residual analysis of earthquake spectral modeling [20] for a number of different events, assuming known source and path propagation effects.

The FAS from the database are then converted into response spectral amplification functions (RSA) using random vibration theory (RVT, [11]) and assuming, as reference input motion, the spectral shape prescribed by the Swiss Ground Motion Model [13,18], a Fourier based ground motion prediction model constrained by ground motions observed from small local and regional earthquakes and by the macroseismic field of the large damaging earthquakes in Switzerland. Since the input motion is highly dependent on the characteristics of the target earthquake, response spectral amplifications from the different methods have been computed for – and grouped into – a variety of magnitude and distance combinations. RSA are initially calculated for the horizontal component only, while the vertical component is subsequently derived from a combination of horizontal-to-vertical conversion relations, both empirical and modeled using a predictive relation based on quarter-wavelength average soil properties [22,36]. This ensures that individual horizontal and vertical ground-motion pairs correspond to the same scenario, rather than being uncorrelated.

As a second step, we produce a database of site-specific Uniform Hazard Spectra (S-UHS) by combining a target Uniform Hazard Spectrum on rock condition (R-UHS; [3]) from the Swiss National Probabilistic Earthquake Hazard Model [19,45] with the set of previously derived response spectral amplification functions. The different curves are grouped and then averaged within each analyzed SIA soil class (Table 1) and for a range of magnitudes and distances compatible with the disaggregation scenario for the region. For the target scenario, we use results from the city of Sion (Switzerland). Sion is considered as representative of one of the areas of high (with respect to the national average) earthquake hazard in Switzerland. Although the calculation is made for different return periods (500, 1000, 5000 and 10,000 years), mean R-UHS are first normalized to peak ground acceleration on rock [42], to allow the subsequent implementation of generic (non-dimensional) site-specific Elastic Design Spectra (S-EDP).

In the following, we will describe in more detail each step of the aforementioned procedure. It must be noted that in the manuscript we often alternate frequency and period representation of spectral quantity. This is done in order to facilitate the separation of information. For example, amplification functions (either Fourier or response spectral) are better presented in frequency domain to highlight features that are relevant in site response analysis such as fundamental frequency of resonance of the soil column. Conversely, hazard and design spectra are generally presented in period, for consistency with the standard engineering representation. Nonetheless, we use a logarithmic scale for both frequency and period axes, which makes them equivalent by simple mirroring.

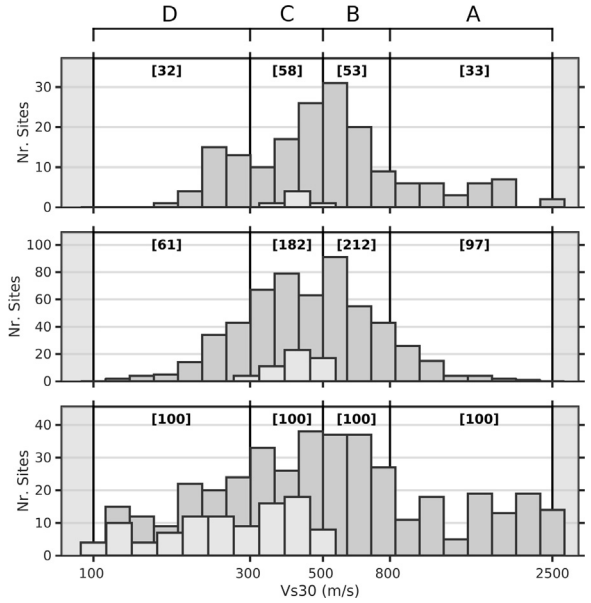

Fig. 2. Distribution of Vs_{30} values of the three available databases for each SIA261 soil class (see Table 1). Swiss sites are on top, Japanese KiK-net network in the middle, while at bottom are the stochastically generated Vs profiles. Class E, whose bounds overlap class C and D, is represented with a separate histogram in foreground with light gray.

3. S-wave velocity profiles

For the calculation of modeled amplification functions, we primarily target the shear-wave velocity profiles available from the Swiss Seismological Service (Schweizerischer Erdbebendienst – SED) site characterization database [41]. However, the number of measured velocity profiles available from the SED database is not sufficient to fully represent the variability of site conditions in all SIA classes (Fig. 2). In particular, class E is poorly represented, mostly due to the present criteria of site selection for the Swiss seismic network. Moreover, several profiles for class A are characterized by a considerable uncertainty, due to the difficulties in performing measurement on rock conditions (particularly when using ambient vibration analysis). To overcome this lack of information, additional datasets have been included in the analysis: the Japanese KiKNet network [4] and a synthetic dataset of stochastically generated S-wave velocity profiles (Fig. 2). In the following, the main characteristics of the three collections are presented and discussed. All profiles from the three datasets, grouped by soil class, are shown in Appendix A.

3.1. The Swiss database

The SED site characterization database consists of a collection of 182 sites investigated using ambient vibration methods (> 150), active seismic techniques (> 50) or both. Some of these sites are at, or close to, the location of a seismic station of one of the Swiss networks (SSMNet and SDSNet). Presently, 67 stations have also velocity profiles at the site of the installation [31,32,39]. An additional 70 stations are planned and will be characterized in the framework of the SSMNet renewal project *Phase II* (2013–2019) [24].

Velocity profiles derived from surface-wave analysis of ambient vibrations are the most reliable and can reach considerable depths (commonly > 100 m), depending on the array size and the maximum resolved wavelength [40], achieved by the combined inversion of surface-wave dispersion curves (both Love and Rayleigh) and Rayleigh wave polarization functions (ellipticity). S-wave profiles investigated with active seismic techniques (MASW) are in few cases less reliable, due to the difficult measuring conditions (mostly in the case of hard rock sites), and the low penetration depth of the method (< 30–35 m), which requires some extrapolation to greater depth [38].

Table 2
Coefficients used in Eq. (1) for the calculation of amplification factors from quarter-wavelength parameters.

Freq. (Hz)	a	b	c	Std. Dev.
0.5000	− 1.22343021	− 0.09253728	9.33123794	1.74583268
0.6071	− 1.11197660	− 0.23564151	8.51657322	1.57108930
0.7372	− 1.06373934	− 0.21171599	8.08744397	1.52088470
0.8952	− 1.10196139	− 0.23563287	8.28666344	1.49371848
1.0870	− 1.09345790	− 0.25167924	8.12311413	1.50346784
1.3200	− 1.03314722	− 0.08190246	7.51212602	1.51062331
1.6028	− 0.99945603	− 0.11252443	7.18289346	1.53062641
1.9463	− 0.93887908	− 0.07426708	6.64489353	1.56715689
2.3633	− 0.82918214	0.14424344	5.67542095	1.64688093
2.8697	− 0.78990921	0.22503225	5.26358993	1.75377631
3.4847	− 0.75058333	0.25561919	4.88743599	1.84644394
4.2313	− 0.72504056	0.27363343	4.61506951	1.89035900
5.1380	− 0.68004352	0.28229386	4.27374641	1.94908695
6.2390	− 0.59734476	0.29105031	3.75415800	2.11275645
7.5759	− 0.58572901	0.38997457	3.54586918	2.14787210
9.1993	− 0.48971738	0.46415892	2.85661243	2.16327385
11.1705	− 0.24196712	0.46821897	1.31263144	2.26742291
13.5641	0.04217755	0.56457828	− 0.53854378	2.45169460
16.4707	0.26928134	0.48532613	− 2.10539861	2.61387313
20.0000	0.31820171	0.36880777	− 2.75905104	2.80810875

3.2. The Japanese KiK-Net database

The Japanese KiK-net strong-motion network [4] includes a collection of velocity profiles (P and S) from 689 sites of the network. These profiles were provided by the Japanese National Research Institute for Earth Science and Disaster Prevention (NIED) and were obtained from downhole logging in boreholes set up for the installation of buried sensors. The KiK-net velocity profiles are often represented with very few (equivalent) layers. This is generally not a problem when long-period ground motion is analyzed, but amplification models at high frequencies can suffer from this oversimplification. This issue will be better developed later in this study. Note also that the KiK-net network includes only a small number of very soft soil conditions due to the site selection criteria.

From the whole dataset with 689 sites, a subset of 607 was analyzed in this study. The sites were selected based on the comparison of empirical amplification functions and H/V spectral ratios with modeled amplification functions from the 1D velocity profiles. For more details about the selection procedure refer to Poggi et al. [36,38].

3.3. The stochastic dataset

A set of stochastically generated velocity profiles has been produced to compensate for the lack of information in specific soil classes, particularly A and E. The randomization process is based on Vs_{30}. For each class, 100 random realization of Vs_{30} are first uniformly generated (Fig. 2) within the bounds prescribed by the soil class definition in SIA 261 normative (Table 1). Subsequently, synthetic velocity profiles are constructed for each given Vs_{30} using a stochastic approach. This approach is advantageous since many profiles with similar (or same) Vs_{30} can be produced, but with generally different velocity distribution over depth, and therefore different site response.

The procedure to generate a synthetic profile for a specific Vs_{30} value is described as follows. For the site class of the target Vs_{30}, a preliminary one-dimensional soil profile is initially generated. S-wave velocity and thickness of each layer are randomly selected within *a-*

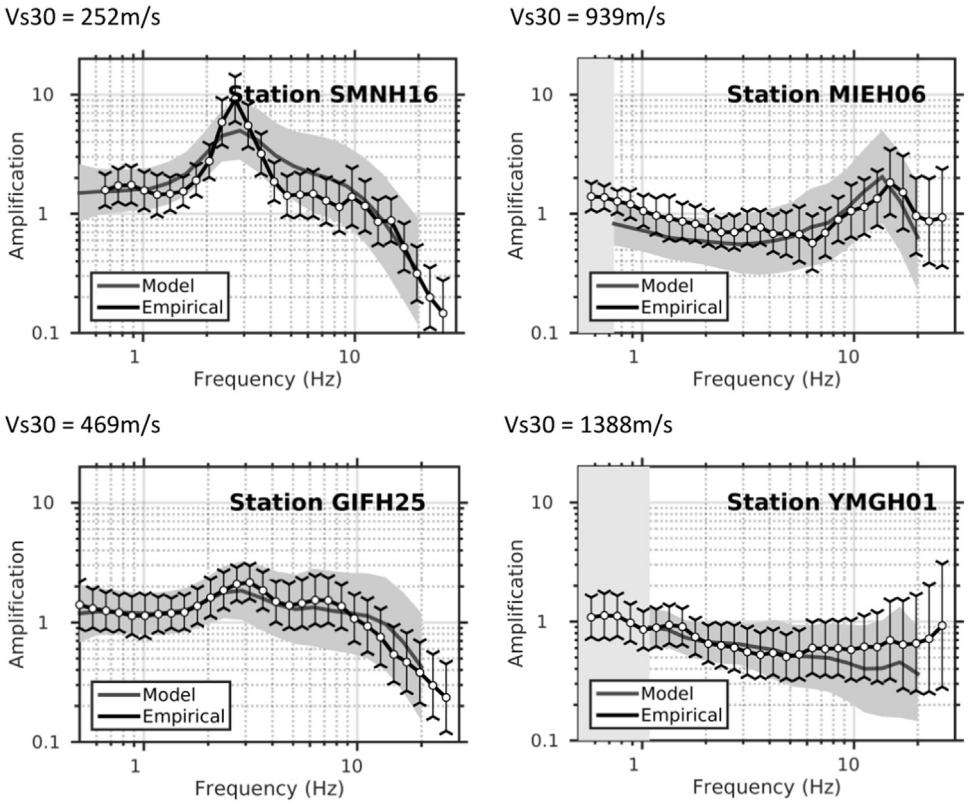

Fig. 3. Comparison between amplification functions from spectral inversion (empirical) and modeling using the quarter-wavelength parameters at four example sites of the Japanese KiK-net network. Vertical bar and gray shaded area represent uncertainty of respectively empirical and modeled curves.

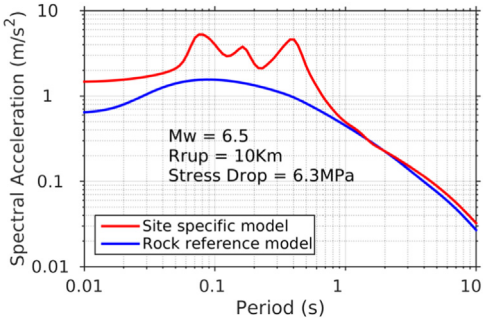

Fig. 4. Example of acceleration response spectra obtained from spectral modeling (using Swiss specific parameterization) and random vibration theory (RVT). The site-specific model is obtained combining the rock-reference spectrum with a FAS amplification from a given database and modeling strategy.

priori bounds depending on the site class, while the number of layer is arbitrary prescribed (in this case ten). As additional conditional constraint, layer's velocities are forced to increase monotonically with depth. Such assumption is nonetheless valid only for the generation of the initial model, but is subsequently relaxed. At this stage, in fact, the Vs_{30} of the generated profile could be quite different from the desired value. In a following step, then, the layer's velocities are iteratively adjusted to progressively match the target Vs_{30}. A linearized optimization algorithm is used for the purpose, where the velocity variations (ΔVs) are the search parameters and the L2 norm of the Vs_{30} (current versus target) is the objective function to be minimized. Because of the non-conditional adjustment, the final profile can include moderate velocity inversions, although the overall shape is usually preserved (see Fig. A3 of the Appendix A).

It has to be noted that for those sites with $Vs_{30} < 800$ m/s, a bedrock interface is also initially accounted in the model by including a variable velocity contrast (of max. 1500 m/s) at random depth location. For class E this interface is forced to range between 5 m and 30 m only and with a velocity of the bedrock not lower than 800 m/s, to match site class definition.

4. Fourier amplification functions

4.1. Empirical amplification

For each real-time station of the Swiss networks (SSMNet, SDSNet) an empirical estimate of the local amplification (both elastic and anelastic) and its related uncertainty are available. Empirical site amplification functions are obtained at each site from a procedure of spectral modeling and inversion of a large number of small-magnitude events [20]. This procedure is a by-product in the development of stochastic ground-motion prediction equation for Switzerland [18,21].

The method consists in the definition of a reference spectrum modeled using the event-specific inverted source characteristics and regional ground-motion attenuation models for each station. The general form of source and path effects can be described through a regional ground motion prediction equation (GMPE) providing the spectral shape at a reference velocity structure as a function of a number of parameters (corner frequency or stress drop, seismic moment and distance, regional Q-model and geometrical spreading model, reference near site attenuation term, etc.). A generalized inversion scheme is needed to derive the different model parameters simultaneously over a large number of stations of the network and a large number of events. The advantage is that for a specific event, the source characteristics are common over the different stations, while for a specific station, site amplification can be considered constant between events of similar characteristic. Such redundancy reduces the non-uniqueness of the inverse problem, giving the possibility to better constrain the model

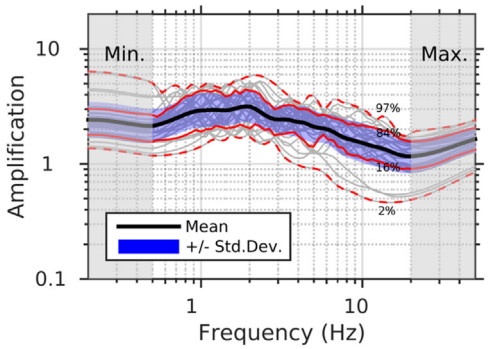

Fig. 5. Mean response spectral amplification (in black) obtained by averaging all curves (in light gray) within a specific soil class. In this example, we present the result for the Swiss database and SIA soil class D, using amplification functions modeled using SH-wave transfer function. Red lines (solid and dashed) represent the different percentiles, while the region within one standard deviation is in blue. Reliability bounds for the calculation are shown in gray.

parameters and minimizing the trade-off with the estimation of the local site-amplification factors, which are then obtained as the residual between observation at the site and modeled spectral shapes at reference rock at the station site.

Same approach was also applied to the stations of the Japanese network. In this case, however, empirical amplifications are referred to different (average) rock reference conditions. While the Swiss reference has a Vs_{30} of about 1100 m/s [35], the Japanese reference is slightly faster (1350 m/s; [38]). To make amplification comparable, then, Japanese spectra have been corrected to Swiss conditions using the frequency-dependent correction procedure in Eq. (6) of Edwards et al. [20].

4.2. QWL amplification model

There have been several studies about the implementation of local amplification predictors based on the comparison between observed empirical amplifications and site-specific proxies. In this study we refer to the method proposed by Poggi et al. [35,36], where a predictive model was calibrated by comparing observed ground motion against average soil proxy parameters computed using the quarter-wavelength (QWL) approach: the average velocity (Vs^{Qwl}) and the impedance contrast (IC^{Qwl}).

The quarter-wavelength average velocity was initially proposed by Joyner et al. [27], and subsequently optimized by Boore [6], and consists of the travel-time average of the elastic parameters down to a depth corresponding to 1/4 of the wavelength of interest. Such estimates are therefore frequency dependent and are suited to be related to the specific site amplification in different frequency bands. Boore did not originally correlate such parameter with actual ground motion observations, which was done subsequently by Poggi et al. [35] for rock sits. However, using the quarter-wavelength average velocity alone is not sufficient to characterize the variability of the ground-motion at soft sediment sites. Spectral amplification induced by resonance is related to the contrast of the seismic impedance at depth. For this reason, we have extended the original idea by introducing the concept of quarter-wavelength seismic impedance contrast [36]. This parameter gives the possibility of directly relating the largest seismic velocity contrasts of a velocity profile with resonance amplification.

The correlation to seismic site response has then been exploited by comparing empirical (anelastic) amplification functions from spectral modeling and quarter-wavelength parameters for a set of selected sites of the Japanese KiK-Net strong motion network. From regression analysis, we derived a simple functional form to predict frequency-dependent amplification factors in the range 0.5–20 Hz at any site with a one-dimensional velocity profile of sufficient depth:

$$A(f) = \exp\{a(f)\log[Vs^{Qwl}(f)] + b(f)\log[IC^{Qwl}(f)] + c(f))\} \quad (1)$$

The values of the frequency dependent coefficients a–c are presented in Table 2. Using this approach, we have modeled anelastic Fourier amplification functions for all the sites of the Swiss and Japanese databases with available velocity profile (e.g. Fig. 3) and for all the synthetic S-wave velocity profiles from the stochastic profile generation.

4.3. SH-wave transfer function

The seismic response of horizontally layered structures can be modeled by approximation of a linear system under SH-component impulse excitation [29], which results in the analytical transfer function of the soil system. In spite of being a rather simple modeling approach, the SH-wave transfer function (SHTF) method provides sufficiently satisfactory results in most cases where a sufficient level of knowledge of the model parameters (velocity, density and quality factors) is available and assuming a negligible influence of other phenomena such as non-vertical incidence of wave, 2D/3D and non-linear seismic response effects. Compared to amplification from direct observations and empirical modeling, SHTF often produces sharp and larger resonance peaks, which can reasonably be considered as uppermost bound of 1D amplification. On the contrary, the deep minima of the theoretical transfer function are less pronounced in observed data. For this reason, keep this theoretical modeling strategy as a mean to map the epistemic variability of our predictions.

Unfortunately, no information about quality factor (Qs) is available. Therefore, we introduced an approximated model to derive quality factors from S-wave velocities, in the form:

$$Qs = (0.01*Vs)^{1.6}+10 \quad (2)$$

Such model is based on the comparison with the high-frequency attenuation decay from the empirical observations, which is quite uncertain, and therefore it should be presently regarded as purely qualitative.

4.4. Using a common reference condition

All amplification functions (measured or simulated) need to refer to a common reference rock Vs-profile that should, in addition, correspond to the rock reference for the regional probabilistic seismic hazard assessment. The use of an incorrect reference condition may lead to over- or underestimation of the final computed seismic hazard. As introduced in Section 4.1, all empirical and numerical amplification functions in this study (in both Fourier and response spectral domains) as well as uniform hazard spectra have been referenced to same ground conditions, which are defined by a gradient s-wave velocity profile with Vs_{30} of 1100 m/s [35] and an average anelastic attenuation model with $\kappa = 0.016$ s [18].

5. Response spectral amplification

5.1. RVT amplification model

Transforming Fourier amplification functions into response spectral amplification functions is a non-linear process. The result depends, other than on the input amplification model, on the definition of a reference ground motion and the corresponding waveforms used for the calculation. As standard practice, a large number of different waveforms are used to produce mean spectra representative of a specific scenario. However, to analyze multiple magnitude and distance combinations, the use of observed waveforms is impractical, mostly due to the limited availability of empirical data (with associated reliable metadata).

To overcome this problem, a stochastic approach based on random

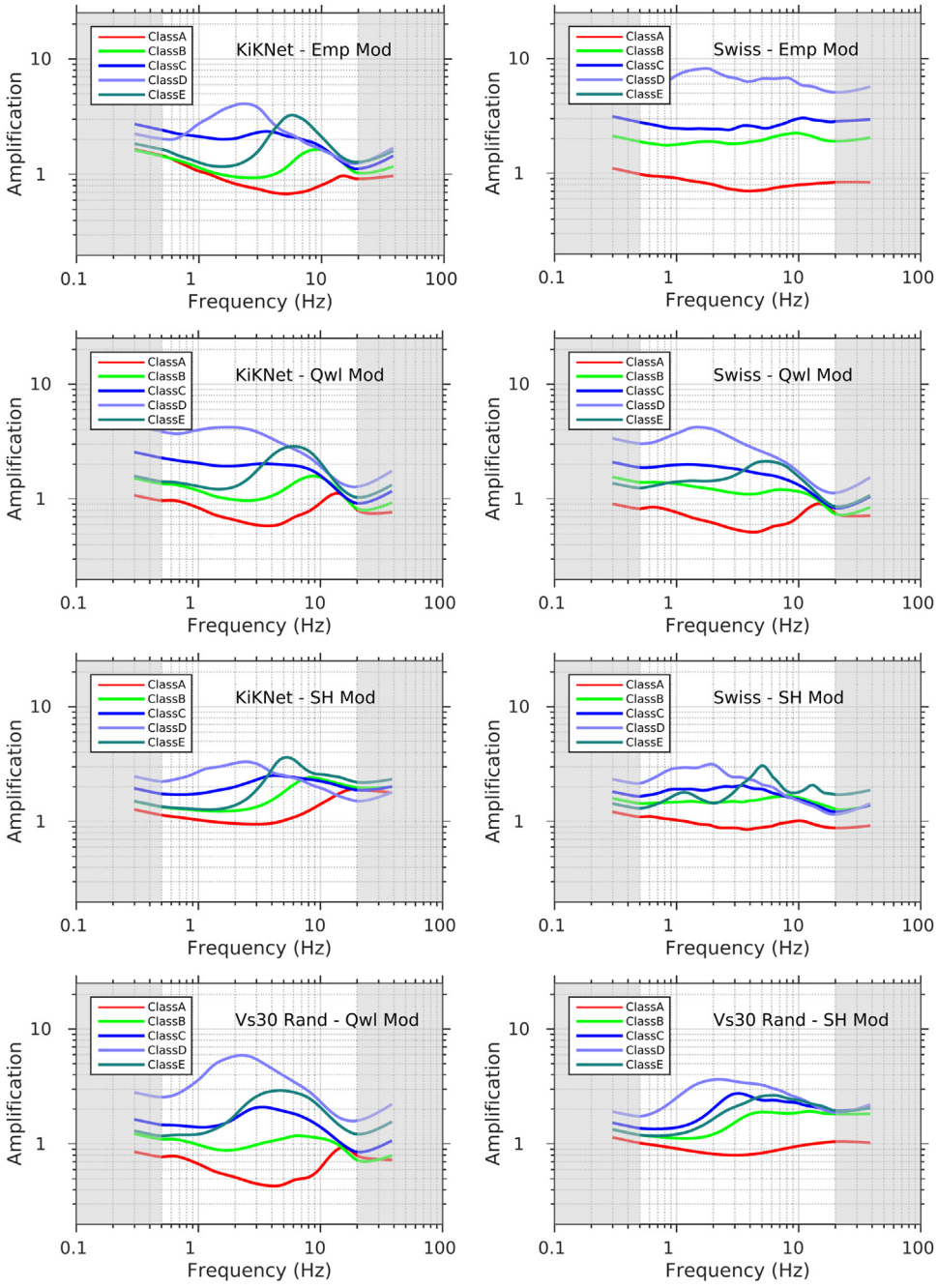

Fig. 6. Comparison of class-specific mean response spectral amplification curves (here for the horizontal component) for different datasets and modeling methods and for a given scenario of $M_W = 6.5$ and $R_{rup} = 10$ km. Unconstrained frequency range is shaded in light gray.

vibration theory (RVT, [11]) can be used to generate "average" response spectral estimates. The method, proposed by Boore [6], is based on the analytical modeling of the input earthquake spectrum by considering source, path and site characteristics. From that, the corresponding *expected* (in a statistical sense) response spectrum is directly computed using RVT. This modeling approach, however, requires the calibration of several parameters that are model (e.g. attenuation, duration) and scenario (e.g. magnitude, distance, stress drop) specific.

To define the reference ground motion of the stochastic modeling we used the parameters of the Swiss spectral model as prescribed by [18] for the alpine region. This is also necessary for consistency with the procedure used to retrieve input empirical Fourier amplification models (see the previous section) and to preserve the referencing to the Swiss reference rock profile [35]. The procedure to compute response spectral amplification functions using stochastic modeling is then two steps (Fig. 4). At first, two response spectra are computed with RVT for a given scenario: the first one including the site-specific amplification (target spectrum) while the second not (the rock reference ground motion). Subsequently, the site-specific spectrum is divided by the rock reference spectrum, to isolate the site component in the response spectral domain.

As major drawback of the method, it is sensitive to some parameters having large uncertainty, such as the duration model. In this study we use the Swiss duration model proposed by Edwards and Fäh [18],

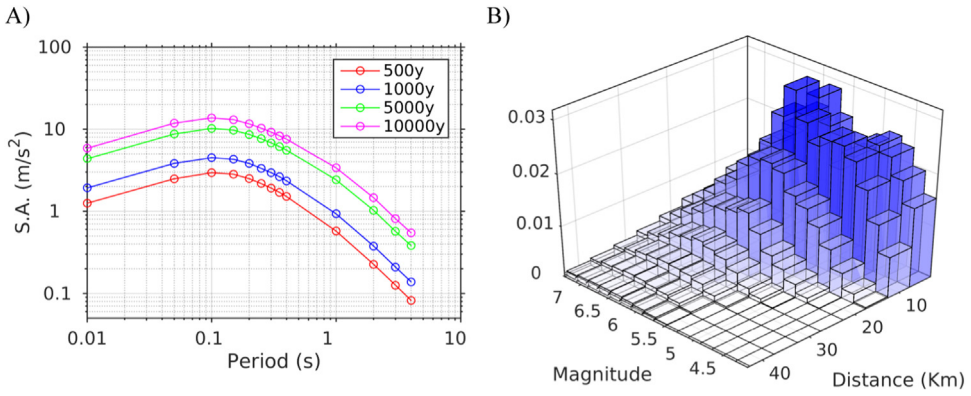

Fig. 7. A) Uniform hazard spectra from probabilistic seismic hazard assessment of the Sion site at different return periods. B) Comparison between magnitude-distance disaggregation scenario at PGA for Sion from the 2016 Swiss probabilistic hazard models at 5 s period (in this example for the return period of 500 years).

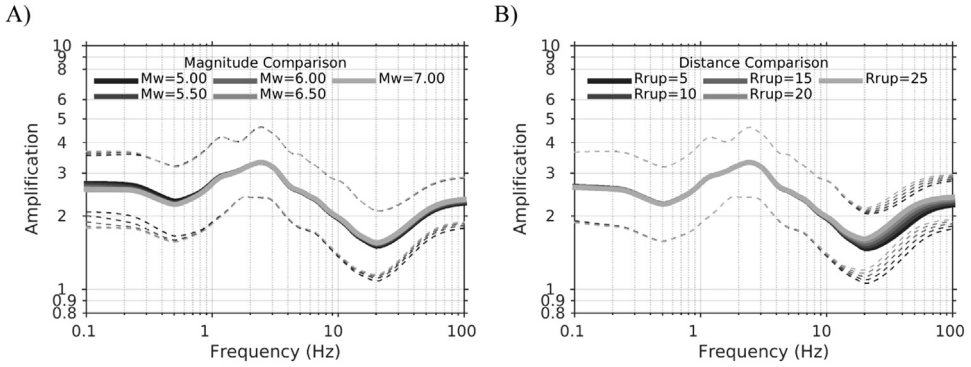

Fig. 8. Example of sensitivity of response spectral amplification functions (Japanese dataset, Class D) with respect to distance (A) and magnitude (B) according to scenarios defined from the disaggregation of the seismic hazard.

which relates the duration of the ground motion to magnitude and distance. However, this model is calibrated on small magnitudes and might introduce some bias in the computation of response spectral amplitudes when used with large magnitudes (> 5), likely leading to some underestimation of the computed ground motion. Such deviation would moreover scale proportionally with the size of the event, making then difficult an absolute quantification.

5.2. Horizontal to vertical conversion

In most cases, response spectral amplification functions for the vertical component are not computed directly but derived from the horizontal models by applying a frequency dependent V/H conversion factor. This approach is largely used in literature (e.g. [33,30]), and it has the advantage to avoid calibrating two separate models for the two components. More importantly, it allows the use of unique disaggregation scenarios [23] consistent between the horizontal and the vertical direction of motion. As a draw back, however, this method suffers the limitation of propagating the variability of the horizontal component and of the V/H conversion factor to the vertical component.

To perform the conversion we use two complementary approaches. The first approach is based on the use of a functional V/H relation to convert directly response spectral ordinates. The functional relation is site-dependent and requires the knowledge of the velocity structure of the site, represented by means of the two quarter-wavelength parameters (average velocity and impedance contrast), as for the case of the empirical amplification model. More details on the study can be found in Edwards et al. [22] and Poggi et al. [36]. The method has been calibrated on soft sediment sites, but as it was shown in Poggi et al. [36], it provides consistent results also in case of stiff soil and rock sites. Conversely, the second approach uses direct V/H spectral ratio observations to correct the Fourier amplification functions *before* the conversion to response spectral ordinates. Being this method based on site-specific observations, it is supposed to generate a smaller uncertainty in the prediction, but on the other hand it has the disadvantage of being applicable only to a restricted number of sites with sufficient earthquake recordings. In this case, the empirical V/H spectral ratios are averaged over events of different magnitude and distance (depending on the availability of data). This however can introduce some additional bias to the prediction that is difficult to assess for all sites of interest and is outside the scope of this study.

6. Comparing modeling strategies

Response spectral amplifications have been computed for all available sites in each SIA class (A to E), database (Swiss, Japanese and stochastically generated profiles), Fourier amplification type (empirical or modeled with QWL approach and SH-wave transfer function) and for different combinations of magnitudes (5–7 with steps of 0.5) and distances (5–25 km with 5 km steps). In total, 71,275 amplification functions are stored in our database for just the horizontal component. From those, mean response amplification functions have then been computed for each soil class separately (e.g. Fig. 5); a total of 1000 mean curves is available for the analysis (see Fig. 6 for an example computed at M = 6.5 and R_{rup} = 10 km).

By comparing the different mean curves for each class, the following characteristics are noticeable:

- With the exception of the Swiss empirical observations, all curves show a similar trend and shape, although with generally different amplification levels;
- Average amplification level in each class is progressively increasing

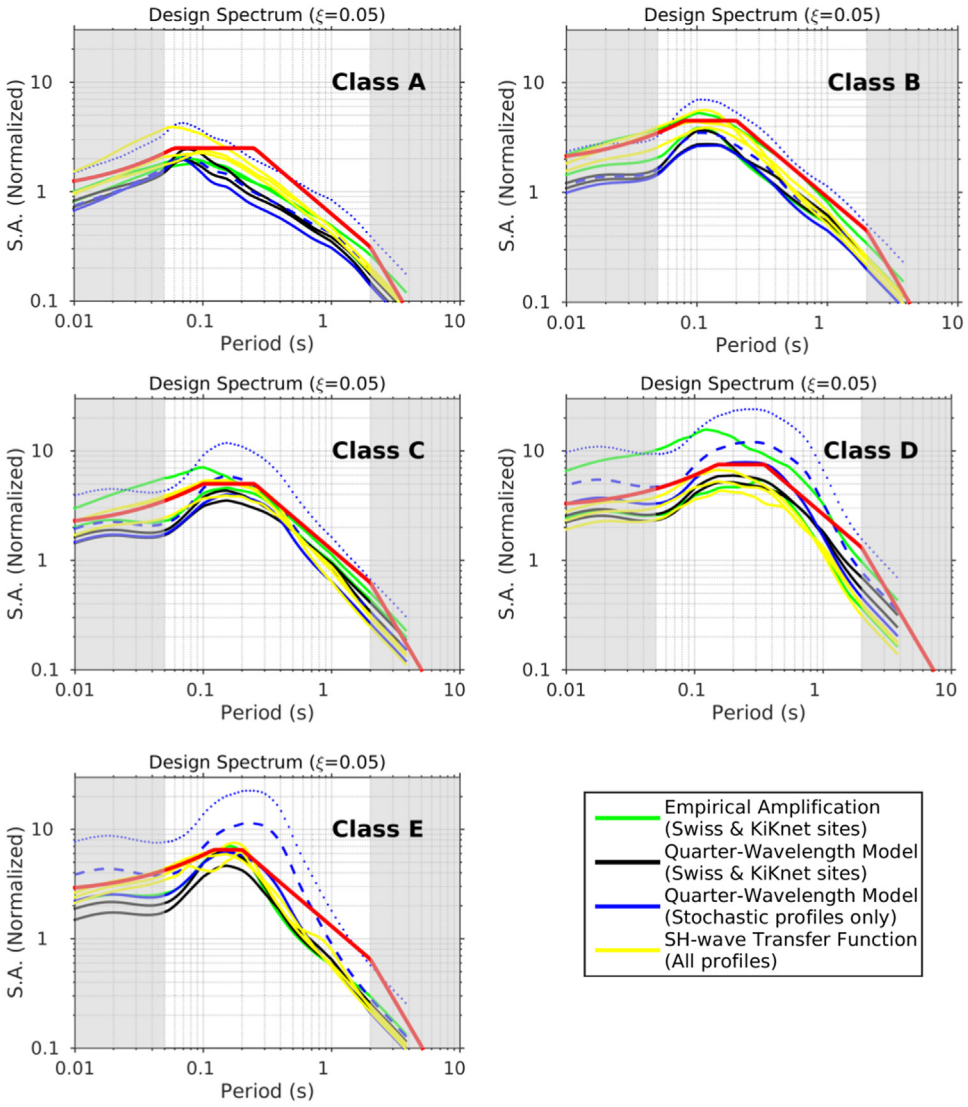

Fig. 9. Normalized spectral acceleration curves for the different SIA class (horizontal component). Different colors represent different approaches to compute amplification. In green are the empirical observations (Switzerland and Japan); in yellow the analytical amplification from SH-wave transfer function; in black the quarter-wavelength amplification models for Switzerland and Japan, while in blue the amplification models from the same model but from stochastically generated velocity profiles (dashed and dotted lines for respectively plus one and two standard deviations, to provide a first order indication of the model variability). Proposed design spectra are in red. Gray areas represent the regions where amplification models are poorly constrained by actual data. The UHS for 500 years return period was used.

Table 3
Values of parameters needed to define the elastic design spectrum (horizontal and vertical component) proposed in this study.

	Horizontal				Vertical			
Class	*S*	T_B [s]	T_C [s]	T_D [s]	*S*	T_B [s]	T_C [s]	T_D [s]
A	1.00	0.06	0.25	2.00	0.65	0.06	0.25	2.00
B	1.80	0.08	0.20	2.00	0.80	0.06	0.25	2.00
C	2.00	0.10	0.25	2.00	1.00	0.07	0.25	2.00
D	3.00	0.15	0.35	2.00	1.60	0.10	0.30	2.00
E	2.60	0.12	0.20	2.00	1.15	0.08	0.20	2.00

from class A to D (as expected);

- The average location of the fundamental frequency of resonance is moving from high to low frequencies between class A and D. Amplification at resonance shows also a consistent trend, with amplitude increasing with decreasing surface average velocity of the site;
- Class A has generally amplification lower than 1. This is due to the proper referencing to the Swiss rock reference profile, which has Vs_{30} lower than many sites in this class; also the very large amplifications at soft sediment classes C and D are due to the referencing;
- Class E represent the most extreme case, being an intermediate stiff soil or rock site, but with a significant resonance amplification at high frequencies. Class E is not represented in the empirical Swiss database but might deserve further investigation;
- The dissimilarity of the Swiss empirical dataset is mostly due to a lack of calibration data (e.g. in class D) and to the fact that some classes are not fully represented by the available stations. For many sites, in particular in class D, ground-motion is largely affected by edge-generated surface waves, typically observed in Alpine valleys. A large difference is also apparent in the attenuation level at high frequencies, which is quite low if compared to Japanese sites.
- QWL amplifications show non-negligible differences compared to SH transfer function results. Among possible explanations, this could be due to the uncertainty in the Q model. For this reason, minor significance is generally given to the SH analytical model for the subsequent calibration of ESP.

7. Seismic hazard input

7.1. Disaggregation scenario

The Swiss Seismological Service provides national support for the implementation, maintenance and dissemination of the probabilistic seismic hazard model for Switzerland. In the present study, we used the

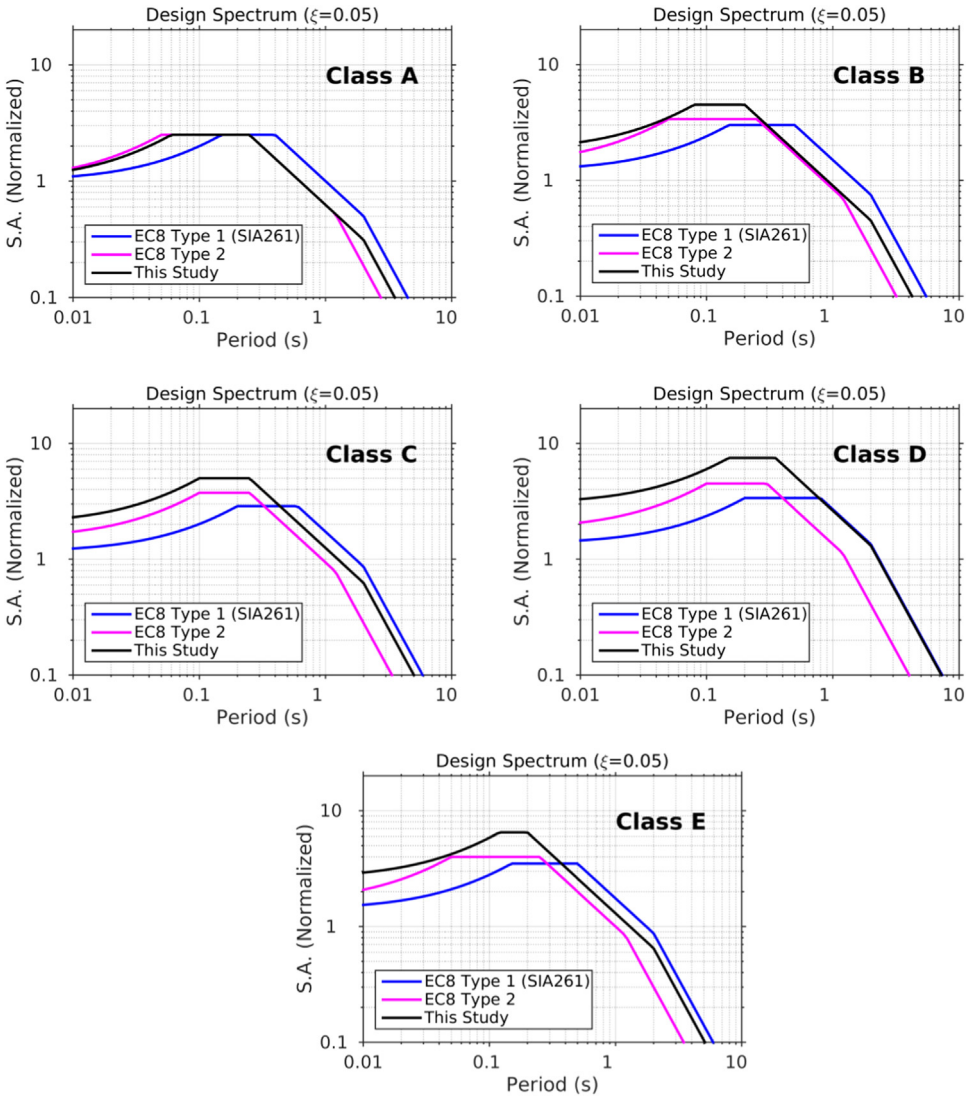

Fig. 10. Comparison between the proposed normalized design spectra for the horizontal component and the design spectra from current normative (SIA261 and Eurocode8).

most recent results from the 2015 revision [45] of the national model. We use as reference for the calculation the uniform hazard spectra (UHS; [3]) in ground acceleration for four significant return periods: 500, 1000, 5000 and 10,000 years (corresponding respectively to the probability of exceedance of 10%, 5%, 1%, and 0.5% in a 50 years observation time). We use in our study the results for Sion, considered representative of the hazard scenario in Switzerland (Fig. 7a) in the highest zone 3b and with the largest values of the design spectrum.

To restrict the number of magnitude-distance combinations to be included in the subsequent computation of the response spectral amplification functions and to avoid the inclusion in the analysis of parameterizations of scarce or no relevance to the total hazard [14], a disaggregation analysis was performed [5]. As can be seen from Fig. 7b, hazard is mostly controlled by the range of magnitude between 5 and 6.5 and distances between about 5 km and 20 km. To add conservatism to the analysis, however, we included in our computations magnitudes up to 7 and distances up to 25 km.

7.2. Testing sensitivity to magnitude-distance

After having selected the range of magnitude and distance of interest from the disaggregation, we proceeded by testing the sensitivity of these M-R combinations to the computed response spectral amplification functions. By comparing results from the different strategies, the influence of the magnitude and distance selection to the variability of site response is only minor (e.g. Fig. 8). This could be a real feature or possibly due to some limitations of the simplified RVT method in modeling spectra, which still needs to be verified against actual recordings.

More in detail, it was possible to observe that magnitude has a (relatively) larger influence at the low frequencies (long periods), while the high frequency part of the amplification spectrum shows more sensitivity to distance. Soil classes with softer sediments, moreover, show a more pronounced variability, although quite minimal if compared to the total uncertainty of the spectral amplification functions. Given these results, it was then decided to use a unique combination of magnitude (6.5) and distance (10 km) for the subsequent analyses. The small variability induced by M-R is nevertheless accounted for by adding a reasoned conservatism to the final elastic design spectra at appropriate periods.

8. Elastic design spectra implementation

Two sets of class-specific design spectra have been implemented

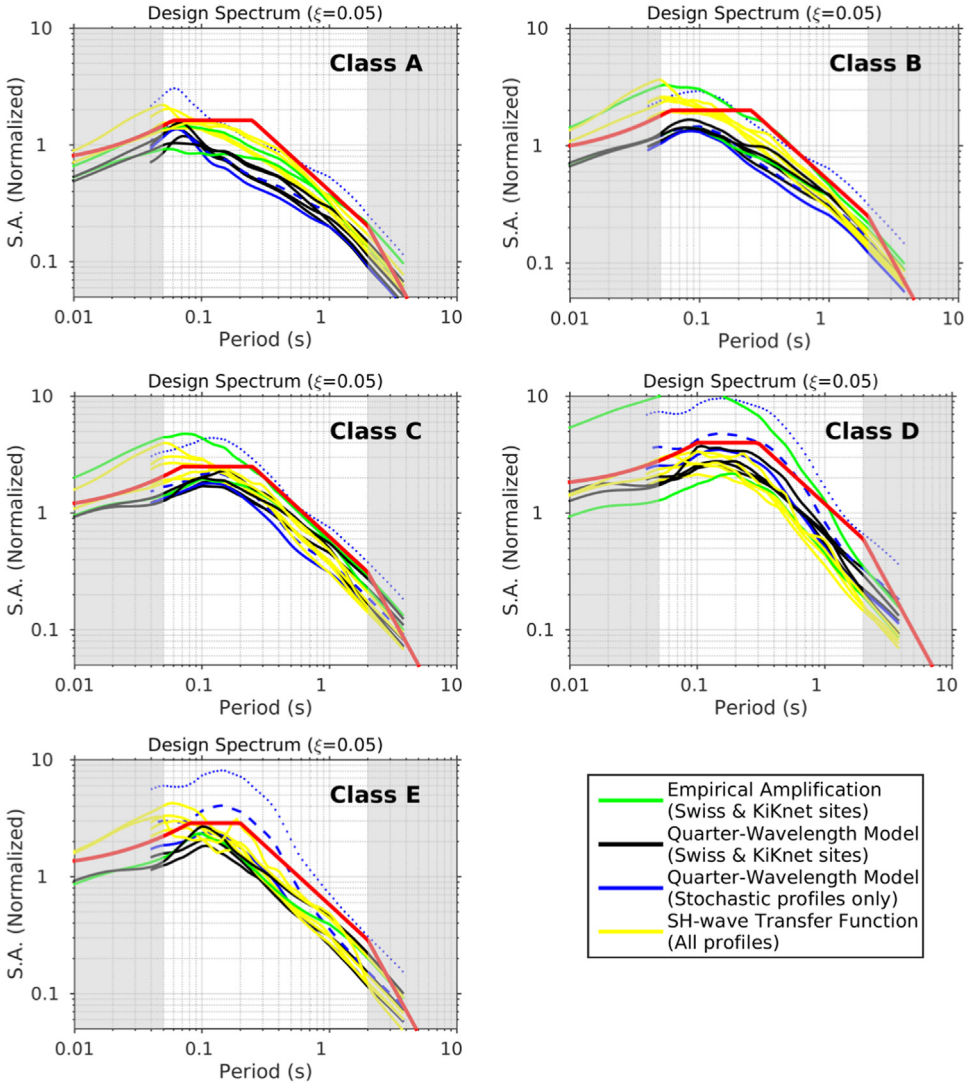

Fig. 11. Normalized spectral acceleration curves for the different SIA class (vertical component). Color scheme is consistent with that in Fig. 9, as described in the caption.

separately for the horizontal and the vertical directions of motion. The proposed design spectra are based on functional forms used in current normatives (SIA261 and Eurocode8). Using the original formulation has the additional advantage of an easy comparison of the proposed shapes with those prescribed by existing building codes. Only the values of the control periods (T_B, T_C and T_D) and the plateau spectral acceleration (S) have been modified to accommodate for the variability of the data available in this study. The functional forms are clearly designed to preserve regions of constant ground motion (displacement, velocity and acceleration) and to avoid divergence of the spectra. The class-specific spectra are meant to be scaled for the peak spectral acceleration defined on reference rock for the specific region and return period.

To implement class-specific design spectra, the ensemble of previously obtained site-dependent uniform hazard curves (UHS) was analyzed. Given the small sensitivity of the response spectral amplification functions to magnitude and distance pairs that are relevant for the disaggregation scenario, a unique combination of magnitude and distance (M = 6.5 and R = 10 km) was used for the definition of the control periods.

Although the spectral curves on rock have been first normalized to the PGA, the variability of the UHS for the different return periods (RP) is nevertheless accounted in the implementation of the design spectra by adding sufficient conservatism at long periods (variable between classes, but up to maximum factor of 0.5 for classes D–E). Is to be noted that normalized design spectra are asymptotic to the class-specific S values only at period 0 s; the S value is not necessarily equal to one for all classes (see Eq. (25) at page 60 of the SIA261 normative), as it is controlled by the site response of the class.

8.1. Horizontal design spectra

To fit the design spectral shapes to the site-dependent spectral acceleration curves, we used a decision-tree approach, providing different significance to the different amplification models according to representativeness of each model to the (expected) mean ground motion level for each class. The different (normalized) spectral acceleration curves for each tested amplification model are presented in Fig. 9 for the 500 year return period

As previously noted, observed amplification functions for Switzerland have a rather high amplification level for those SIA soil classes corresponding to soft sediment sites. This is due to the location of these stations within the Swiss strong motion network. In many cases the observed ground motion is likely affected by phenomena such as geometrical effects, 2D/3D resonances and edge generated surface waves that could introduce significant amplification (e.g. in case of deeply incised alpine valleys, see Michel et al. [31]). An impartial

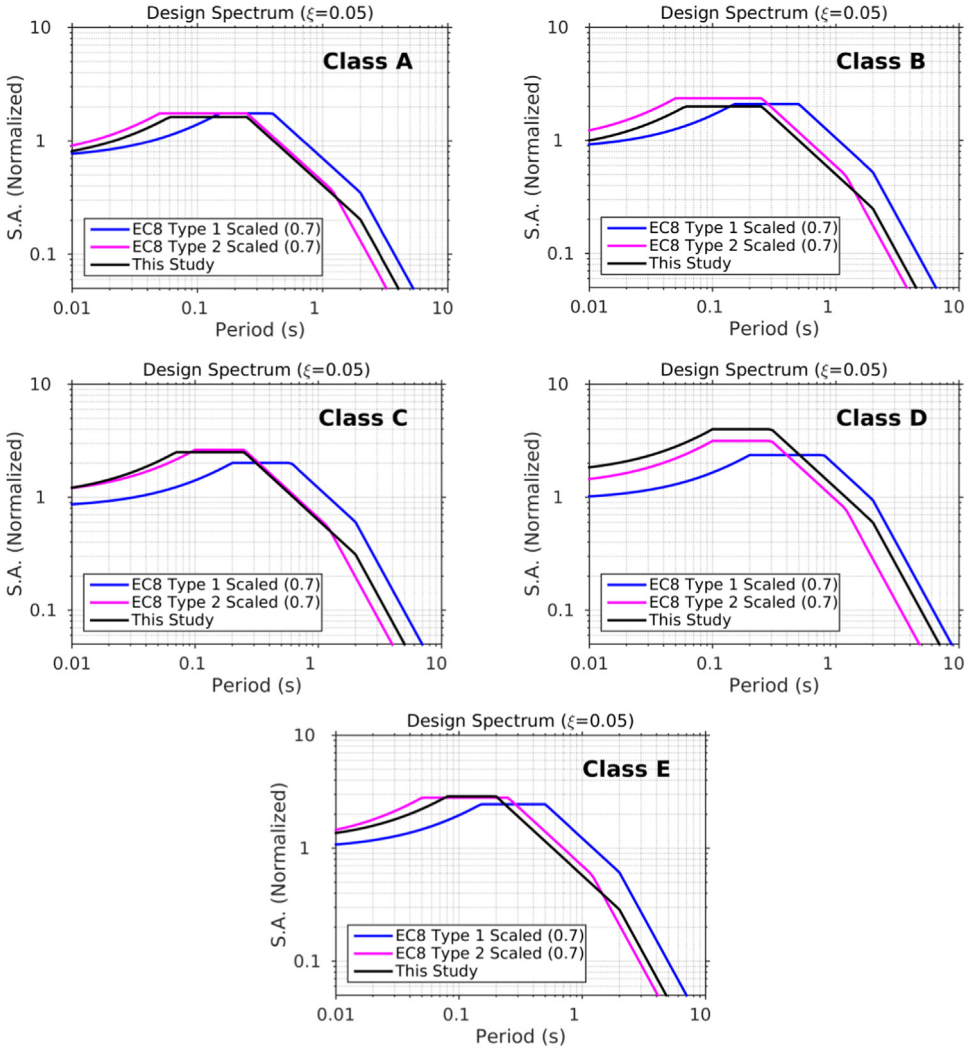

Fig. 12. Comparison between the proposed normalized design spectra for the vertical component and the horizontal design spectra from current normative (SIA261 and Eurocode8) scaled by the standard factor of 0.7.

quantification of these phenomena, however, is at present stage still challenging. Convincing criteria to account for such effects into design is not yet available and their related variability should be therefore considered as purely epistemic.

To fit the design spectrum, several criteria were considered, beyond the simple enveloping of the available curves. In the long periods we accounted for the effect of different return periods on the hazard. In this region, the design shape is consistently above the different site-dependent models. In addition, the control periods T_D is imposed to be equal to 2 s for all classes. The values for the control periods and plateau acceleration for the horizontal component are presented in Table 3.

With respect to the elastic acceleration design spectra from the current SIA normative (Fig. 10) the proposed shapes have generally higher amplitudes of the plateau (below about 0.5–0.6 s) for all classes, with the exception of class A. These large amplitudes are related to the development to resonance phenomena in sediment sites (stiff and soft), which are dominant in the intermediate-to-high frequency range of the site amplification functions. Conversely, the proposed model has a design amplitude generally lower than prescribed by the SIA normative for long periods. For soil class A and B, its shape is in this range more similar to the *Type 2* spectra of the Eurocode (recommended for small to moderate magnitude events; Ms < 5.5).

8.2. Vertical design spectra

For the definition of the elastic design response spectra for the vertical component, we first applied the approach prescribed by the SIA normative (Section 16.2.3.2), which consists in reducing the shape of the class-specific horizontal component by a factor of 0.7. This approach provides a design shape quite conservative with respect to the vertical models, where at some periods the amplitudes are largely overestimated. We therefore proceeded also with the implementation of separate design spectrum by defining a new set of control parameters. The values for the control periods and plateau acceleration for the vertical component are presented in Table 3.

The selection criteria were similar to those used for the horizontal component, with the additional constraint of keeping the design of the horizontal and vertical shapes as consistent and comparable as possible (Fig. 11). In more detail, the vertical design spectrum for class A is in agreement with that obtained by scaling the horizontal component by constant factor. For all other classes, however, the newly proposed shapes are, in most cases, below their scaled counterpart. The value of 0.7 appears therefore to be conservative for sediment classes, as the vertical component is likely affected by resonance phenomena, but not as significantly as the horizontal. In our opinion, this provides clear

evidence that class-dependent design should be always preferred, as it could better represent the variability on the vertical motion in case when dealing with local soil conditions.

Moreover, by comparing the proposed design spectrum with the Eurocode spectra (horizontal shape scaled by the factor 0.7) it is possible to observe similarity of our model with the *Type 2* spectra (Fig. 12), except for soil class D. The agreement is for both the long-period flank amplitudes and particularly for the plateau level. This observation provides evidence that *Type 2* spectral model could be to a certain extend better representative of the Swiss conditions for the vertical component, in particular for the short period range.

9. Discussion and conclusions

We propose a new set of coefficients for the implementation of soil class specific design spectral shapes for both the horizontal and the vertical components. The proposed models have been calibrated on normalized uniform hazard spectra (UHS) from the probabilistic seismic hazard assessment at Sion (Switzerland). To account for the variability of site response in different soil conditions, a set of mean response spectral amplification functions (observed and modeled) was defined for the different soil classes and applied to the UHS. The proposed design spectral shapes have a functional form consistent with the present normative, but they differ from them in terms of controlling periods (T_B, T_C and T_D) and plateau level (S).

By comparing the proposed shapes with current normative spectra, some relevant features are noticeable. For the horizontal component, the long period part of the developed acceleration spectrum is generally lower than SIA design spectrum, but always between the shapes of *Type 1* (equivalent to SIA) and *Type 2* spectra of the Eurocode. At intermediate to short periods (high frequency region, where resonance phenomena are relevant in soft sediment sites), the plateau amplitude is consistently above the present normative, and also generally higher than the EC *Type 2* spectrum. When using the functional form defined in EC8, the large plateau amplitudes have the drawback of imposing an increased acceleration at PGA. A possible solution would be to use a different equation for the design spectrum at short periods (before T_B) with steeper amplitude decay. This needs however further discussion. The conservative choice of a *Type 1* spectrum in the present SIA code at long periods might be desirable, also accounting for near-source effects such as source directivity. However at short periods, the *Type 1* spectrum is not sufficiently conservative. A combination with a spectrum as proposed in our study or a spectrum similar to EC *Type 2* should be discussed. Regarding the vertical component, the recipe prescribed by SIA normative (scaling for a factor 0.7) can be accepted, although it turned out to be a conservative choice for all spectral ordinates. If a reduction of the level of conservatism is targeted, however, the proposed model might be preferred.

Appendix A. Velocity profiles

See Figs. A1–A3.

Additional issues raised during this study are related to the soil classes defined in the normative. In particular, we observed that a classification scheme based on the use of Vs_{30} only is too simplistic, as also questioned by other studies (e.g. [12,28]). Large resonance amplifications occur in almost all classes (B–D) and are a clear indication that large averaging of resonance amplification effects occurs over different frequency bands. To reduce such variability (and therefore the model uncertainty) a classification scheme that includes *also* the use of the fundamental frequency of resonance of the site (f_0, measured or calculated) would be advisable. Class E is a very special class of difficult identification that is presently not well represented in the data set for Switzerland. The use of the fundamental frequency of resonance of the site (f_0) would also help in this case.

Some sites might be influenced by special phenomena, such as 2D/3D resonance and edge-generated surface waves, which can increase the amplitude of ground motion by large factors. This is typically the case in Switzerland for deeply incised alpine valleys. Although there is presently no sufficiently general way to quantify the contribution of these phenomena other than performing targeted site-specific investigations, their influence should be better accounted for in the future normative, e.g. by introducing ad-hoc scaling procedures calibrated on geometrical proxies. Complementary, the effect of soil non-linearity should also be properly considered in the predictive model, having likely an impact on the variability of the spectral values at short periods (and thus S), particularly for classes D to E and long return periods, which are controlled by events of size capable of triggering non-linear response on the soils. Non-linearity is therefore also an important future target of our research.

Lastly, some features of our model could be improved with additional scientific research. The duration model developed for Switzerland might not account properly for the effects of very soft sediment sites, where the generation of long period surfaces wave might lead to increased shaking duration. This would also have a direct impact on the amplitude level of the response spectral amplification functions. Near-surface damping (in term of attenuation parameter *kappa*) is still poorly constrained in many cases; this leads to very large uncertainties in the prediction of high frequency ground-motion amplification. There is a need for new methods for a better estimation of the site attenuation term, either by direct measurement or from the definition of innovative site-specific proxies.

Acknowledgments

This study was supported by the Swiss Federal Office for Energy (SFOE) in the context of the renewal of the building code for dams. A special thanks goes also to the anonymous reviewers for their appreciation for our work and their insightful suggestions.

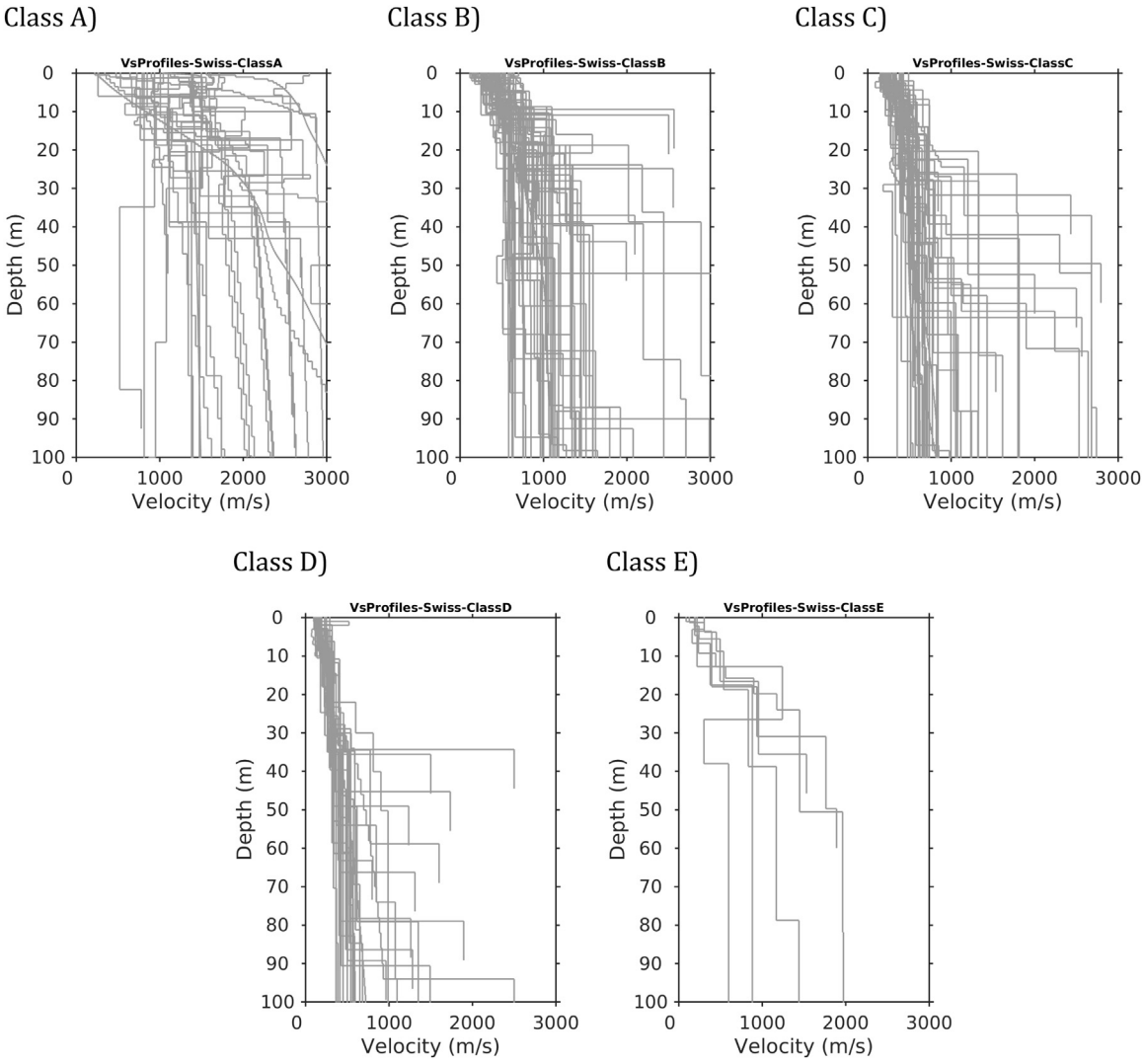

Fig. A1. Comparison of the 182 S-wave velocity profiles from the SED site-characterization database grouped in different SIA soil classes.

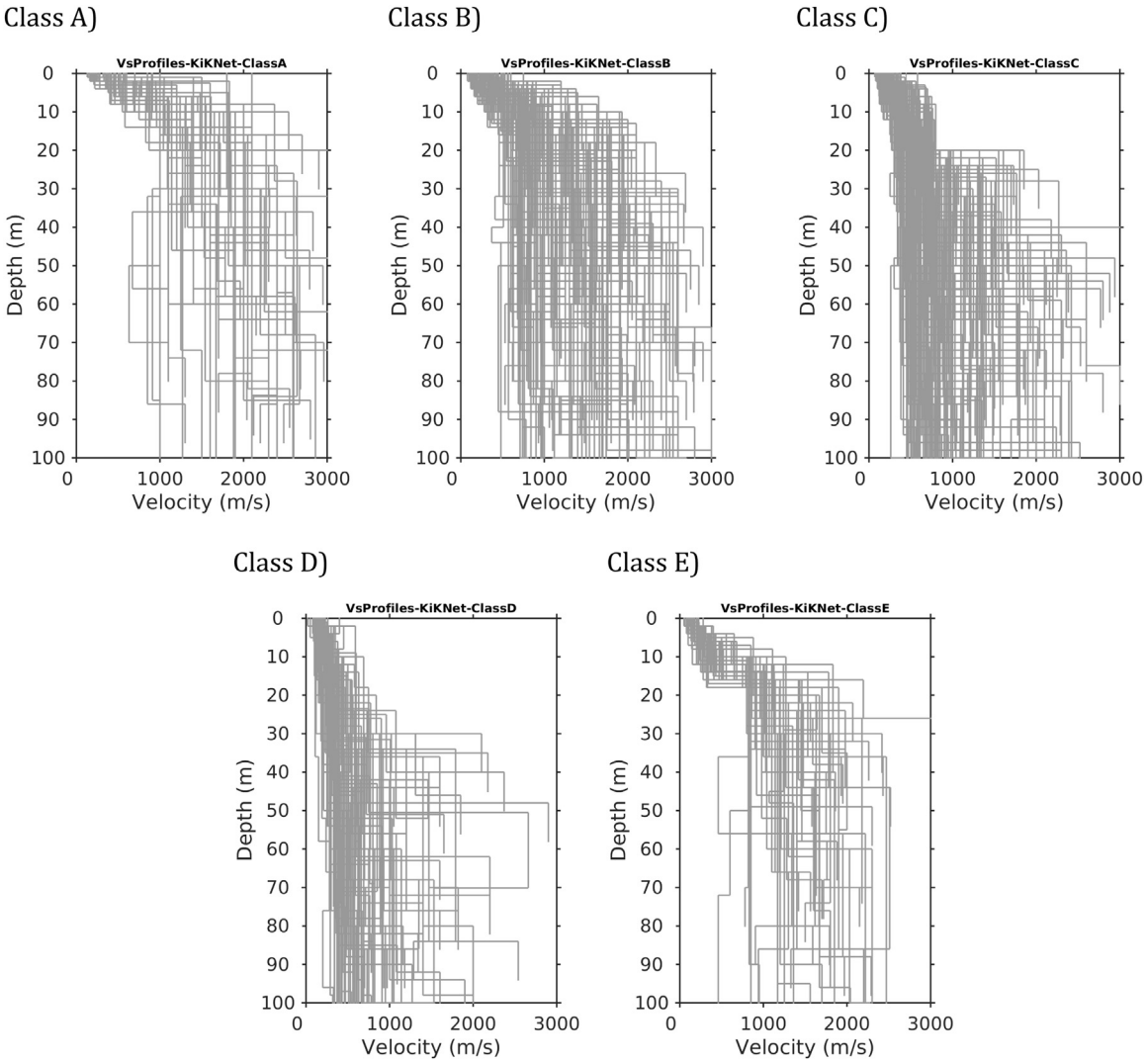

Fig. A2. Comparison of the 607 S-wave velocity profiles selected from the Japanese KiK-Net strong motion database grouped in different SIA soil classes.

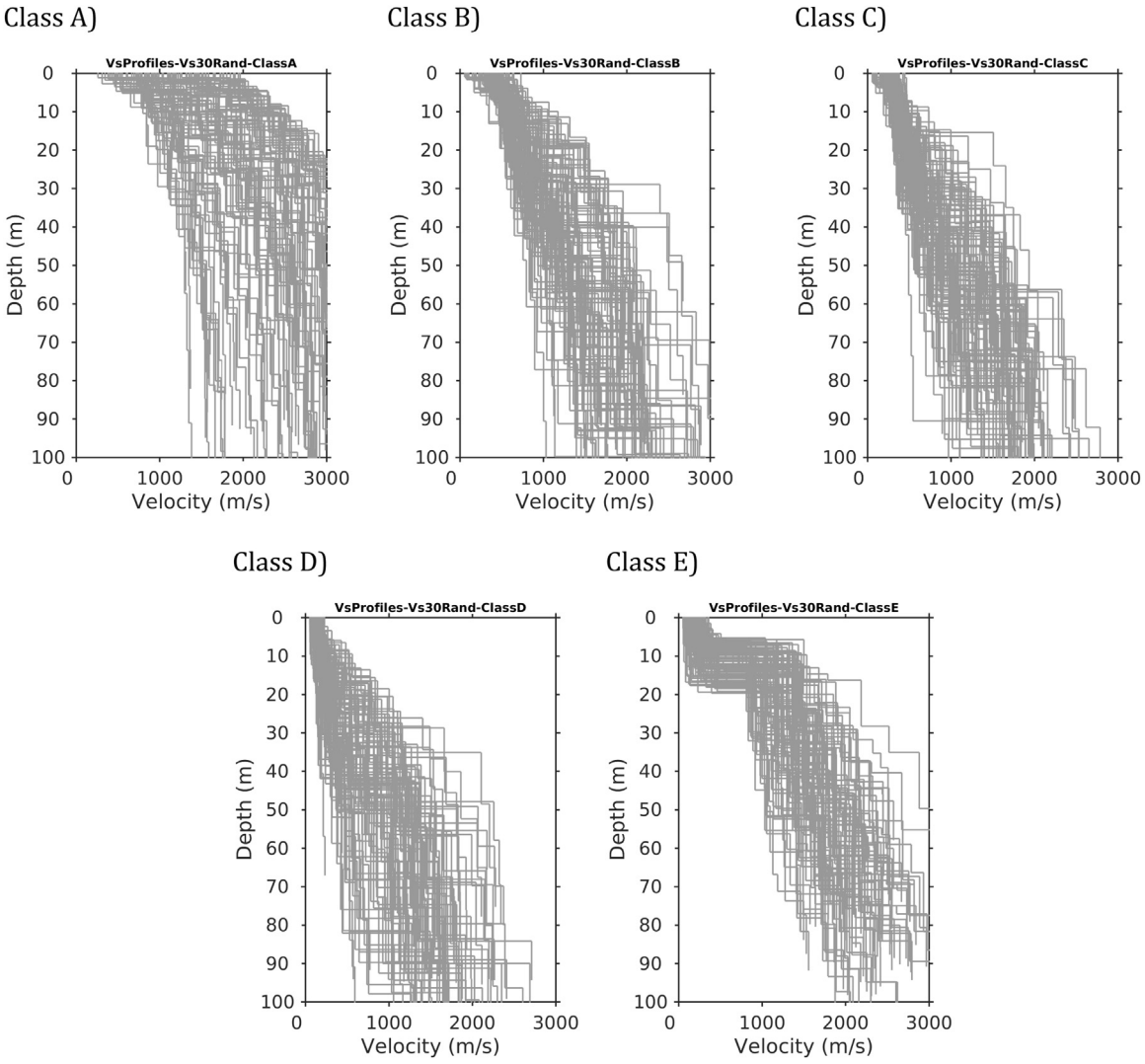

Fig. A3. Comparison of the 500 stochastically generated S-wave velocity profiles grouped in different SIA soil classes.

References

[1] Abrahamson NA. Non-stationary spectral matching. Seismol Res Lett 1992;63:30.
[2] Al Atik L, Abrahamson N. An improved method for nonstationary spectral matching. Earthq Spectra 2010;26(3):601–17.
[3] Anderson JC, Trifunac MD. Uniform risk absolute acceleration spectra. Adv Civ Eng Eng Mech ASCE 1977:332–5.
[4] Aoi S, Kunugi T, Fujiwara H. Strong-motion seismograph network operated by Nied: k-net and kik-net. J Jpn Assoc Earthq Eng 2004;4:65–74.
[5] Bazzurro P, Cornell AC. Dissagregation of seismic hazard. Bull Seismol Soc Am 1999;89(2):501–20.
[6] Boore D. Simulation of ground motion using the stochastic method. Pure Appl Geophys 2003;160:635–76.
[7] Bommer JJ, Scott SG, Sarma SK. Hazard-consistent earthquake scenarios. Soil Dyn Earthq Eng 2000;19:219–31.
[8] Bommer JJ, Acevedo AB. The use of real earthquake accelerograms as input to dynamic analysis. J Earthq Eng 2004;8(S1):43–91.
[9] Borcherdt RD. Estimates of site-dependent response spectra for design (methodology and justification). Earthq Spectra 1994;10:617–53.
[10] BSSC (Building Seismic Safety Council). NEHRP recommended provisions for seismic regulations for new buildings and other structures, Part 1: provisions, FEMA 368. Washington, D.C.: Federal Emergency Management Agency; 2003.
[11] Cartwright DE, Longuet-Higgins MS. The statistical distribution of the maxima of a random function. Proc. R. Soc. London 1956;237:212–32.
[12] Castellaro S, Mulargia F, Rossi PL. Vs_{30}: proxy for seismic amplification? Seismol Res Lett 2008;79:540–3.
[13] Cauzzi C, Edwards B, Fäh D, Clinton J, Wiemer S, Kästli P, et al. New predictive equations and site amplification estimates for the next-generation Swiss shakemaps. Geophys J Int 2015;200:421–38.
[14] Chapman MC. A probabilistic approach to ground-motion selection for engineering design. Bull Seismol Soc Am 1995;85:937–42.
[15] CEN (European Committee for Standardization). Eurocode 8: design of structures for earthquake resistance, Part 1: general rules, seismic actions and rules for buildings. EN1998-1:2004. Brussels, Belgium; 2004.
[16] Choi Y, Stewart JP. Nonlinear site amplification as function of 30 m shear wave velocity. Earthq Spectra 2005;21:1–30.
[17] Dobry R, Borcherdt RD, Crouse CB, Idriss IM, Joyner WB, Martin GR, et al. New site coefficients and site classification system used in recent building seismic code provisions. Earthq Spectra 2000;16:41–67.
[18] Edwards B, Fäh D. A stochastic ground-motion model for Switzerland. Bull Seismol Soc Am 2013;103:78–98.
[19] Edwards B, Cauzzi C, Danciu L, Fäh D. Region-specific assessment, adjustment and weighting of ground motion prediction models: application to the 2015 Swiss seismic hazard maps. Bull Seismol Soc Am 2016. http://dx.doi.org/10.1785/0120150367.
[20] Edwards B, Michel C, Poggi V, Fäh D. Determination of site amplification from regional seismicity: application to the Swiss national seismic networks. Seismol Res Lett 2013;84:611–21.
[21] Edwards B, Fäh D, Giardini D. Attenuation of seismic shear wave energy in Switzerland. Geophys J Int 2011;185:967–84.
[22] Edwards B, Poggi V, Fäh D. A predictive equation for the vertical to horizontal ratio of ground-motion at rock sites based on shear wave velocity profiles: application to Japan and Switzerland. Bull Seim Soc Am 2011;101(6):2998–3019.
[23] Gülerce Z, Abrahamson N. Vector-valued probabilistic seismic hazard assessment for the effects of vertical ground motions on the seismic response of highway bridges. Earthq Spectra 2010;26:999–1016.
[24] Hobiger M, Fäh D, Scherrer C, Michel C, Duvernay B, Clinton J, et al. The renewal project of the Swiss strong motion network (SSMNet). In: Proceedings of the 16th world conference on earthquake engineering (16WCEE). Santiago de Chile; 2017.
[25] Housner GW. Behavior of structures during earthquakes. J Eng Mech Div 1959;85(4):109–30.

[26] ICC. International building code. Falls Church, VA: International Code Council; 2009.
[27] Joyner WB, Warrick RE, Fumal TE. The effect of quaternary alluvium on strong ground motion in the Coyote Lake, California, earthquake of 1979. Bull Seismol Soc Am 1981;71:1333–49.
[28] Lee VW, Trifunac MD. Should average shear-wave velocity in the top 30 m of soil be used to describe seismic amplification? Soil Dyn Earthq Eng 2010;30:1250–8.
[29] Kennett BLN, Kerry NJ. Seismic waves in a stratified half space. Geophys J R Astr Soc 1979;57:557–83.
[30] McGuire RK, Silva WJ, Costantino CJ. Technical basis for revision of regulatory guidance on design ground motions: hazard and risk-consistent ground motion spectra guidelines [NUREG/CR-6728]. Washington, D.C.: U. S. Nuclear Regulatory Commission; 2001. p. 213.
[31] Michel C, Edwards B, Poggi V, Burjánek J, Roten D, Cauzzi C, et al. Assessment of site effects in Alpine regions through systematic site characterization of seismic stations. Bull Seism Soc Am 2014;104(6):2809–26.
[32] Michel C, Fäh D, Edwards B, Cauzzi C. Site amplification at the city scale in Basel (Switzerland) from geophysical site characterization and spectral modelling of recorded earthquakes. Phys Chem Earth Parts A/B/C 2017;98:27–40.
[33] Newmark NM, Hall WJ. Earthquake spectra and design, EERI monograph 3. Oakland, California: Earthquake Engineering Research Institute; 1982. p. 103.
[34] Pitilakis K, Riga E, Anastasiadis A. Design spectra and amplification factors for Eurocode 8. Bull Earthq Eng 2012;10:1377–400.
[35] Poggi V, Edwards B, Fäh D. Derivation of a reference shear-wave velocity model from empirical site amplification. Bull Seism Soc Am 2011;101:258–74.
[36] Poggi V, Edwards B, Fäh D. Characterizing the vertical to horizontal ratio of ground-motion at soft sediment sites. Bull Seism Soc Am 2012;102:2741–56.
[37] Poggi V, Edwards B, Fäh D. The quarter-wavelength average velocity: a review of some past and recent application developments. In: Proceedings of the 15th WCEE. Lisbon, Portugal; 2012.
[38] Poggi V, Edwards B, Fäh D. Reference s-wave velocity profile and attenuation models for ground-motion prediction equations: application to Japan. Bull Seism Soc Am 2013;103:2645–56.
[39] Poggi V, Burjánek J, Michel C, Fäh D. Seismic site-response characterization of high-velocity sites using advanced geophysical techniques: application to the NAGRA-Net. Geophys J Int 2017;210(2):645–59.
[40] Rix GJ, Leipski EA. Accuracy and resolution of surface wave inversion. Am Soc Civ Eng 1991:17–32.
[41] SED – Swiss Seismological Service, ETH Zurich. The site characterisation database for seismic stations in Switzerland. Zurich: Federal Institute of Technology; 2016. ⟨http://dx.doi.org/10.12686/sed-stationcharacterizationdb⟩ retrieved on 04/02/2016 from. ⟨http://stations.seismo.ethz.ch⟩.
[42] Seed HB, Ugas C, Lysmer J. Site-dependent spectra for earthquake-resistant design. Bull Seismol Soc Am 1976;66(1):221–43.
[43] SIA 261:2014. Actions on structures. Swiss Standard SIA 261. Zurich: Swiss Society of Engineers and Architects; 2014.
[44] Trifunac MD. Earthquake response spectra for performance based design—a critical review. Soil Dyn Earthq Eng 2012;37:73–83.
[45] Wiemer S, Danciu L, Edwards B, Marti M, Fäh D, Hiemer S, et al. Seismic hazard model 2015 for Switzerland (SUIhaz2015), Swiss seismological service (SED) at ETH Zurich. Technical report. 2016. http://dx.doi.org/10.12686/a2.